Lump Circuits Elements Values Extraction of Acoustic Transducers Using Impedance Measurement Approach

Yeong-chin Chen [1], Lon-chen Hung[2], Shuh-Han Chao1[2], Tseng-hsu Chien[1]

[1] Department of Computer Science and Information Engineering, Diwan University
No.87-1, Nanshi Li, Madou Township, Tainan County 72153, Taiwan
ycchenster@gmail.com

[2] Department of Electrical Engineering, Diwan University

Abstract: - Acoustic transducers are the popular elements for sonar array. The transducer of the simplify electrical equivalent circuit is discussed, and a impedance measurement system is developed to estimate the elements value of transducer's lump circuit model at or near resonance. For practial application, a matching transformer is designed to make the transducer a high efficiency and high power transmitter. The experiment result approves the. Impedance Measurement Approach is the effective method for high power acoustic transducer development

Key-Words: - lump circuits, Elements values extraction, Acoustic transducers, Impedance measurement

1 Introduction

Piezoelectric material have been utilized in a large variety of applications such as NT&SD Transducer [1], Acoustic Sensor [2], and ultrasonic imaging [3]. In sonar system, Electro-Acoustical transducer is utilized as the physical element for sound wave transmitting and receiving. By transmitting a sound wave from the transducers, the surface or underwater objects ranging several miles away from the sonar transducers can be located by detecting the reflected sound wave from the objects themselves. For high power application, the transducer is typically structured like a "Tonpiltz", composed of head and tail masses, a central prestress rod and piezoelectric-ceramic segments, to produce reinforced mechanical motion of high-power sound generation. Detailed discussion of these longitudinal vibrators may be found in literature [4-8]. However, Tonpiltz transducer possesses characteristics of high dielectric resistance and capacitance and is hard to be driven by the electrical amplifier. In practical applications, a self-coupling transformer is implemented to link the electrical driving system and the transducer to improve the transmitting efficiency.

First, an equivalent circuit based on lumped constant mode [9,10] is proposed as an analogy to electromechanical characteristics of the Tonpiltz transducer. Then, the circuit elements were deduced from the impedance properties of the transducer. A PC-based automatic testing system is built to measure the transducer's properties.

Since the testing program is programmed by Hp-Vee [11] software, the matching transformer is also designed and simulated using the same software. First, the transducer's impedance is measured and the circuit element of equivalent circuit is deduced from the measured data. Then the matching transformer is developed to meet the specifications of impedance matching and high power operation. The impedance properties of the matched transducer could be obtained from the testing system and as a reference to the transformer design. The Hp-Vee possesses a programming capability as the traditional software, but has a better communication feasibility on GPIB and RS232 interfaced instrument than other software. The simulation and measurement are accomplished in the same software by actually reducing the times for trial and errors.

2.Measurement Algorithm

2.1 Lump circuit modeling of Tonpiltz Transducer

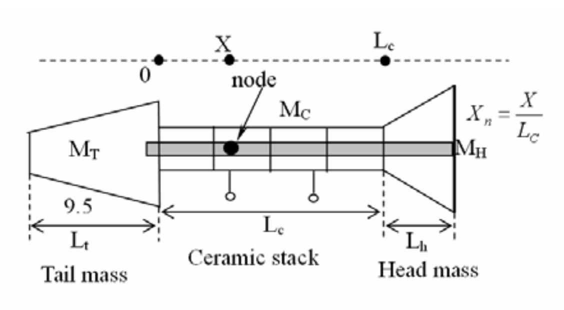

Fig. 1 Tonpiltz transducer cross-section

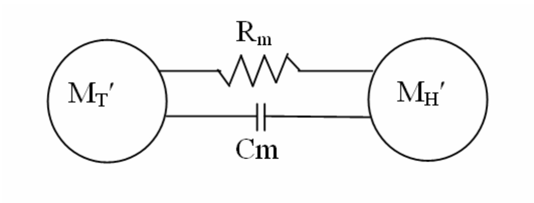

Fig. 2 Simple spring-mass model.of Tonpiltz Transducer.

A cross-section of the Tonpiltz transducer is shown in Fig. 1, along with the simplest spring-mass idealization [12]. The device consists of a stack of eight PZT4 ring transducer elements electrically in parallel, a steel tail mass, a flared aluminum head mass and a steel compression bolt. The transducer can be modeled as simple spring-mass system, shown as Fig. 2. Sphere volume in the spring-mass model indicates relative lumped mass of the tail, M'_T, and head, M'_H, for the device. The mechanical compliance and vibration loss of ceramic segments are indicated by R_m and C_m individually.

If the transducer is vibrating longitudinally in the fundamental mode, there exists a node, X_n, where the vibrating displacement is zero at all times. If friction loss and other mechanical losses are ignored, according to the "conservation of energy" theorem, the node can be derived [13] and the effect tail mass and head mass is expressed by

$$M'_T = M_T + M_C X_n,$$
$$M'_H = M_H + M_C\left(1 - X_n\right) \quad (1)$$

where M_H is head mass, M_C is mass of ceramic segments, and M_T is tail mass.

The equivalent network of the Tonpiltz transducer is described in Fig. 3, where the electrical system is composed of clamped capacitance (C_0) and dielectric resistance (R_0), the mechanical system is composed of the spring-mass model described in Fig. 1, and N_C (Newton/voltage) is the electromechanical transformation ratio between the electrical and mechanical systems. Reducing the mechanical portion of Fig. 3, the equivalent circuit of the transducer is simplified as shown in Fig. 4,

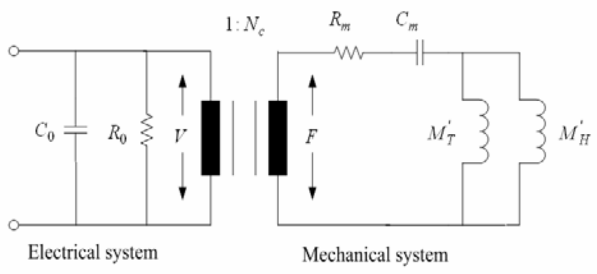

Fig. 3 Equivalent circuit of Tonpiltz transducer working in air.

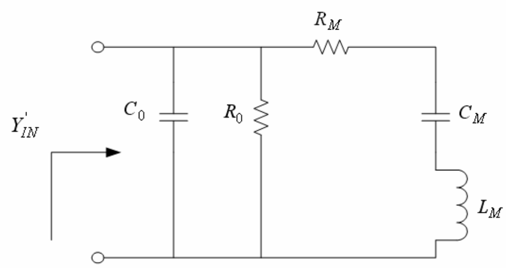

Fig. 4 Simplified equivalent circuit of Tonpiltz transducer.

2.2 Elements Values Extraction of Transducers Lump Circuit

The input electrical admittance of Fig. 4 can be written as:

$$Y_{IN} = Y_E + Y_M = \frac{1}{R_0} + j\omega C_0 + \frac{1}{R_M + j(\omega L_M - \frac{1}{\omega C_M})} \quad (2)$$

where Y_E is electrical admittance, Y_M is mechanical admittance, R_0 is dielectric resistance, C_0 is clamped capacitance, R_M is motional resistance, L_M is motional inductance, C_M is motional capacitance.

In some specific frequency range, the real and imaginary parts of the input electrical admittance can be calculated and plotted in the complex plane [14,15] as in Fig. 5.

The circuit elements in Fig. 4 can be deduced from the specific parameters in Fig. 5, and expressed as below [16,17]:

$$R_0 = \frac{1}{\omega C_T tan\delta} = MIN[Re(Y_{IN})] \tag{3}$$

$$G_S = \frac{1}{R_M} + \frac{1}{R_0} \approx \frac{1}{R_M} \tag{4}$$

$$B_S = \omega_S C_0 = 2\pi f_S C_0 \tag{5}$$

$$f_S = \frac{1}{2\pi\sqrt{L_M C_M}} \tag{6}$$

$$f_P = \frac{1}{2\pi\sqrt{L_M (C_M \| C_0)}}$$

$$C_M \| C_0 = \frac{C_M C_0}{C_M + C_0} \tag{7}$$

$$K_{eff}{}^2 = \frac{f_P{}^2 - f_S{}^2}{f_P{}^2} = \frac{C_M}{C_M + C_0} = \frac{C_M}{C_T} \tag{8}$$

where C_T is electrical capacitance of transducer at DC, $\tan\delta$ is dielectric loss of piezoelectric ceramic, G_S is electrical conductance at motional resonance, B_S is electrical susceptance at motional resonance, f_S is the motional resonance frequency, f_p is the parallel resonance frequency, K_{eff} is the effective electromechanical coupling factor.
Equation (8) gives:

$$C_0 = C_T(1 - K_{eff}{}^2) \quad , \quad C_M = C_T K_{eff}{}^2 \tag{9}$$

This equation explains the relationship between the effective electromechanical coupling coefficient (K_{eff}) and the clamped capacitor (C_0)and motional capacitor (C_M).

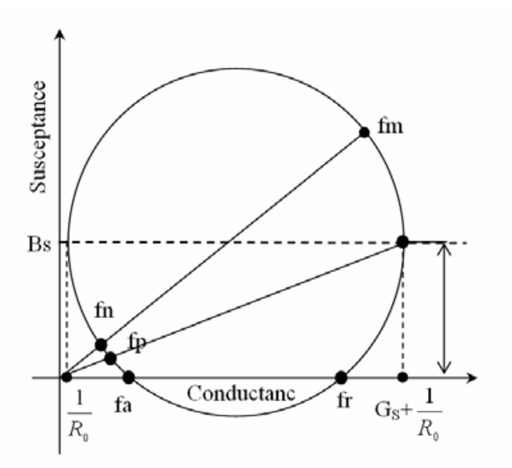

Fig. 5 Complex plane of admittance.

2.3 Impedance Matching Design

In underwater applications, a self-coupling transformer [18], as shown in Fig 6, is implemented to link the electric system and the transducer where it works at resonance frequency. By tuning the secondary inductance value (L_T) and the turns ratio of the transformer, the phase angle (θ) of the transducer's impedance is tuned to zero and the impedance value ($|Z_{IN}|$) is also modified to match the electric driving system so as to improve the transmitting efficiency.

The electrical admittance of the resonating transducer after tuning becomes:

$$(Z_{IN})^{-1} = Y_{IN} = [\,j\omega_S C_0 + \frac{1}{j\omega_S L_T} + \frac{1}{R_M + j(\omega_S L_M - \frac{1}{\omega_S C_M})}](\frac{n_1 + n_2}{n_1})^2$$

$$= \frac{1}{R_M}(\frac{n_1 + n_2}{n_1})^2 \tag{10}$$

The primary inductance (L_1) and the secondary inductance (L_T) has the relation given by:

$$L_T = [\frac{n_1 + n_2}{n_1}]^2 L_1 \tag{11}$$

where n_1 and n_2 are winding turns of L_1 and L_2 respectively. The secondary inductance L_T is used to cancel out the clamped capacitance and make the phase angle zero, and

$$\omega_S{}^2 = \frac{1}{C_0 L_T} \tag{12}$$

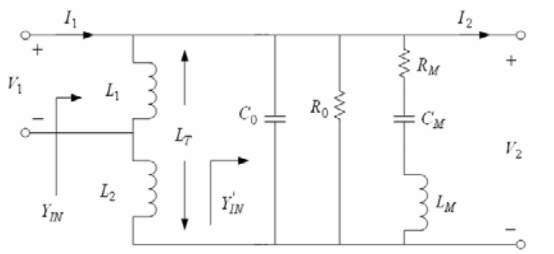

Fig. 6 Equivalent circuit of Tonpiltz transducer with matching transformer.

2.4 Simulation

A circuit with a serial impedance Z is shown as in Fig. 7. Referring to Kirchhoff's laws, the voltage and current relations of input (V_1, I_1) and output(V_2, I_2) in Fig. 7 can be given by

$$\begin{bmatrix} V_1 \\ I_1 \end{bmatrix} = \begin{bmatrix} 1 & Z \\ 0 & 1 \end{bmatrix} \begin{bmatrix} V_2 \\ I_2 \end{bmatrix} \tag{13}$$

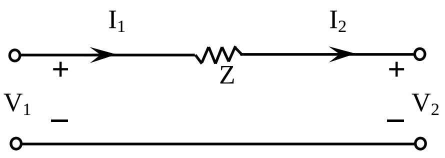

Fig. 7 Circuit with serial impedance.

Similarly, the voltage and current relations of input (V_1, I_1) and output(V_2, I_2) in the shunt impedance circuit, shown as in Fig. 8, can be given by

$$\begin{bmatrix} V_1 \\ I_1 \end{bmatrix} = \begin{bmatrix} 1 & 0 \\ \frac{1}{Z} & 1 \end{bmatrix} \begin{bmatrix} V_2 \\ I_2 \end{bmatrix} \tag{14}$$

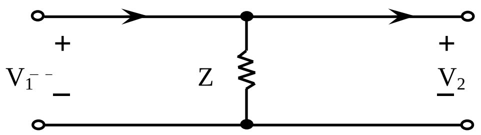

Fig. 8 Circuit with shunt impedance.

For a self-couplinf mode transformer, shown in Fig.9, the currents of loop 1 and 2 is denoted by I_1 and I_2 individually.

Referring to Kirchhoff's voltage laws In loop 1, the voltage V_1 is described by the following equation

$$V_1 = j\omega\,(I_1 - I_2)L_1 - j\omega I_2 M \tag{15}$$

Where $j\omega I_2 M$ is the reverse electro-magnetic voltage built by cyrrent I_2, and M is the mutual coupling inductance between L_1 and L_2 shown as

$$M = k\sqrt{L_1 L_2}\ . \tag{16}$$

For the same reason, the loop equation in loop 2 will be

$$V_2 = j\omega\ I_2\,L_2 - j\omega\,(I_1 - I_2)M + j\omega\,(I_2 - I_1)L_1 + j\omega\,I_2 M \tag{17}$$

Due to equs. (15), (16) and (17) and the couplinf coefficient k is assumed to be 1 , we have the equatin

$$\begin{bmatrix} V_1 \\ -V_2 \end{bmatrix} = \begin{bmatrix} j\omega L_1 & -j\omega(M+L_1) \\ -j\omega(M+L_1) & j\omega(L_1+L_2 M) \end{bmatrix} \begin{bmatrix} I_1 \\ I_2 \end{bmatrix} \tag{18}$$

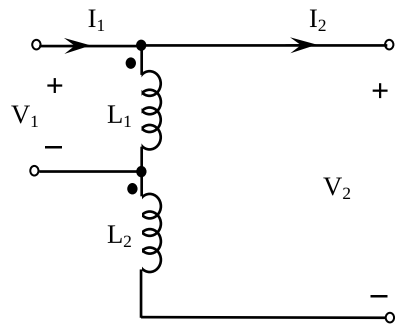

Fig. 9 Self-coupling transformer.

And then

$$\begin{bmatrix} V_1 \\ I_1 \end{bmatrix} = \begin{bmatrix} \frac{L_1}{M+L_1} & \frac{\omega^2(L_1 L_2 - M^2)}{-j\,\omega(M+L_1)} \\ \frac{1}{j\omega(M+L_1)} & \frac{L_1+L_2+2M}{M+L_1} \end{bmatrix} \begin{bmatrix} V_2 \\ I_2 \end{bmatrix} \tag{19}$$

For an ideal transformer

$$M = k\sqrt{L_1 L_2} = \sqrt{L_1 L_2} \tag{20}$$

And

$$\frac{L_1}{L_2} = \left(\frac{N_1}{N_2}\right)^2 \tag{21}$$

where N_1 and N_2 is the wind-turns for inductances L_1 and L_2 sepreatedly.

Equation (19) is simplified as

$$\begin{bmatrix} V_1 \\ I_1 \end{bmatrix} = \begin{bmatrix} \frac{N_1}{N_1+N_2} & 0 \\ 0 & \frac{N_1+N_2}{N_1} \end{bmatrix} \begin{bmatrix} 1 & 0 \\ \frac{1}{j\omega\ L_T} & 1 \end{bmatrix} \begin{bmatrix} V_2 \\ I_2 \end{bmatrix} \tag{22}$$

where the relation of L_T and L_1 is given as

$$L_T = \left(\frac{N_1+N_2}{N_1}\right)^2 L_1\ . \tag{23}$$

According to the networking theorem, the voltage and current relations of input (V_1, I_1) and output(V_2, I_2) in Fig. 6 can be given by:

$$\begin{bmatrix} V_1 \\ I_1 \end{bmatrix} = \begin{bmatrix} n_1/(n_1+n_2) & 0 \\ 0 & (n_1+n_2)/n_1 \end{bmatrix} \begin{bmatrix} 1 & 0 \\ 1/j\omega L_T & 1 \end{bmatrix} \begin{bmatrix} 1 & 0 \\ j\omega C_0 + 1/R_0 & 1 \end{bmatrix} \begin{bmatrix} 1 & 0 \\ 1/(1/j\omega C_M + R_M + j\omega L_M) & 1 \end{bmatrix}$$

$$\begin{bmatrix} V_2 \\ I_2 = 0 \end{bmatrix} = \begin{bmatrix} S_{00} & V_2 \\ S_{10} & V_2 \end{bmatrix} \quad (24)$$

From eq. (24), the input impedance plot can be calculated from:

$$Z_{IN} = \frac{V_1}{I_1} = \frac{S_{00}}{S_{10}} \quad (25)$$

by sweeping the frequency of the input AC signal.

Since V_1 is the input voltage, and V_2 is $V_2 = \frac{V_1}{S_{00}}$, the electromechanical efficiency (η) is estimated by

$$\frac{V(R_r)}{V_1} = \frac{\dfrac{(V_2 \times \dfrac{R_r}{j\omega(M_H{}' + M_W) + R_r})^2}{R_r}}{\dfrac{V_1^2}{Z_{in}}}$$

$$= \frac{1}{S_{00} * S_{10}} \times \frac{R_r}{(j\omega(M_H{}' + M_W) + R_r)^2} . \quad (26)$$

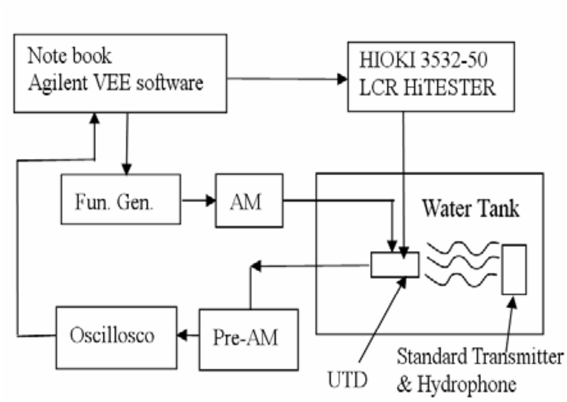

Fig. 7 Diagram of PC_base Measurement Syste.

3 PC_base Measurement System Using Agilent VEE

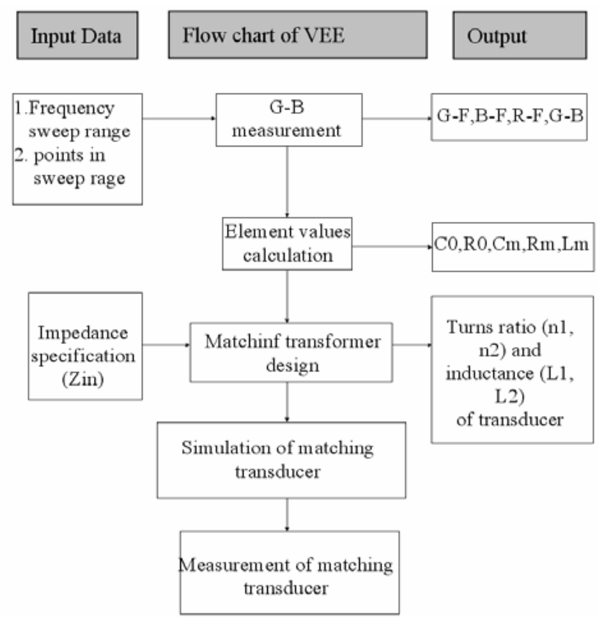

Fig. 8 Flow chart of Agilent VEE Program.

For an underwater high power electro-acoustical transducer, the maximum operating power ($P_{\max}$) is 800W, impedance value (Z_{IN}) at resonant frequency (3.3 kHz) is 145Ω and the phase angle(θ) is ±10°. The experimental procedure is described in the following section.

The hardware set-up of the PC_base Measurement System is shown as in Fig.7. And the program flow chart of VEE program is illustrated in Fig.8.

4 Results and Discussion

Figures 9 show the program view in Agilent VEE. Figures 10 and 11 show the impedance value and phase angle of transducer, before and after impedance is matched, individually. Before impedance tuning, the impedance value is 5.3kΩ@3.3kHz, and the phase angle is -61°@3.3kHz. In VEE program a matching transforer is designed and the simulated impedance values are 144.5Ω@3.3kHz, the phase angle is 1°@3.3kHz. After the matching transformer is built and mounted on the transducer, the transducer shows that the measured impedance values is 141Ω@3.3kHz, the phase angle is -7°@3.3kHz, which met the specifications. In Fig. 10, the simulated data (dash line) agrees the measured data (solid line) very well. The impedance curve shows a peak at about 2.9 kHz which is attributed to the resonance phenomena between the secondary inductance of the matching transformer (L_T)

and the clamped capacitance (C_0).

The power handling capability of the matching transformer is verified by measuring the primary inductance (L_1) and quality factor (Q_1) depending on varied current level as the secondary port of the transformer is circuitry opened. The deviation of primary inductance and quality factor is less than 1% as the current level varies from 0.5 A to 3 A. The secondary inductance (L_T) and quality factor (Q_T) is also measured in the same way as those of the primary with LCR meter (HIOKI 3532-50) by varying the secondary current from 0.05 A to 0.3 A.

The contribution of this research is to propose an impedance measurement of electro-acoustical transducer and to derive the parameters of the lumped-element equivalent circuit of the transducer. Based on the lumped equivalent circuit, the matching theorem is applied to design the transformer and predict the transducer's performance using Agilent-VEE software program. The power capability for the transformer design is also considered in this research. The simulation results approve the effectiveness of this lumped-circuit model of the transducer. The fact that the measurement and simulation are processed in the same software environment reduced the time for trial and errors.

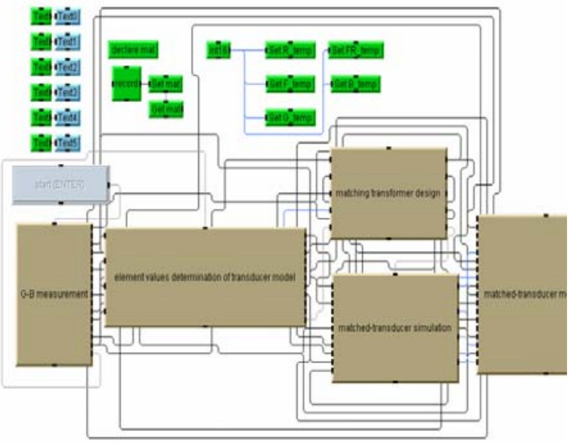

Fig. 9 Main program.

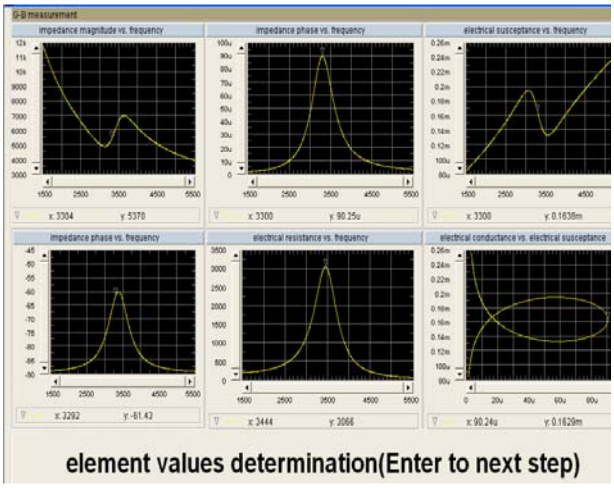

Fig. 10 G-B measurenent for unmatching Transducer.

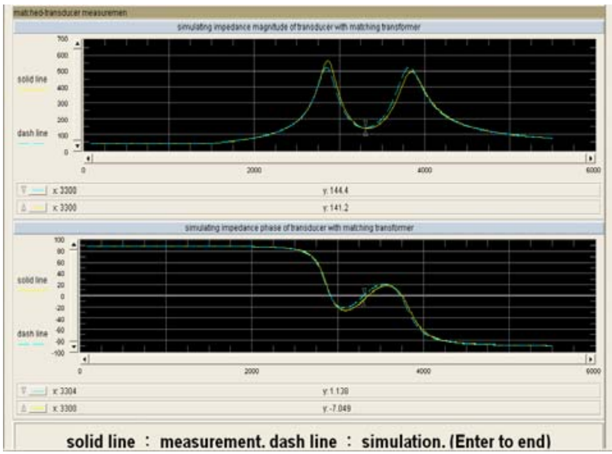

Fig. 11 Matching transducer measurement.

Acknowledgement

This research was supported by the National Science Council of Taiwan, under grant No. NSC96-2815-C-434-001.

References:

[1] S. S. Lin, H. Chang, C. C. Kuo, Y. Su, A New Design NT&SD Transducer Used for Earthquake Detecting System Through Network Communication, *WSEAS Transactions on communications*, Issue 5, Vol. 5, 2006, pp. 766-773.

[2] S. Saleh, H. Elsimary, A. Zaki, S. Ahmad, Design and Fabrication of Piezoelectric Acoustic Sensor, *WSEAS Transactions on Electronics*, Issue 4, Vol. 3, 2006, pp. 192-196.

[3] K. Boumchedda, A. Ayadi, M. Hamadi, G. Fantozzi, Evaluation of Porous PZT with 3-3 Connectivity for Biomedical Ultrasonic

Imaging Applications, Proceedings of the 6th *WSEAS Int.Conf. on Applications of Electrical Engineering (AEE'07)*, Istanbul , Turkey, May 27-29, 2007, pp. 192-196.

[4] C. E. Martin, On The Theory of Segmented Electromechanical Systems, *The Journal of The Acoustical Society of America*, Vol. 36, No. 7, 1964, pp. 1366-1370.

[5] R. Krimholtz, D. A. Leedom, and G. L. Matthaei, New Equivalent Circuits for Elementary Piezoelectric Transducers, *Electronics Letters*, Vol. 6, No. 13, June 1970, pp. 398-399.

[6] D. F. Mccammon, The Design of Tonpiltz Piezoelectric Transducers Using Nonlinear Goal Programming, *J. Acoust. Soc. Am.*, Vol. 68, No. 3, Sept. 1980, pp. 754-757.

[7] T. Inoue, T. Sasak, T. Miyama, K. Sugiuchi, S. Takahashi, Equivalent Circuit Analysis for Tonpiltz Piezoelectric Transducer, *The Transactions of The IEICE*, Vol. E 70, No. 10, October 1987, pp. 909-917.

[8] P. T. Gough, J. S. Knight, Wide Bandwidth, Constant Beamwidth Acoustic Project: A simplified Design Procedure *IEEE Ultrasonics Symposium* , 1992, pp. 341-358.

[9] Y. C. Chen, S. Wu, A Design Approach of Tonpiltz Transducer, *Japanese Journal of Applied Physics*, Vol. 41 , Part 1, No. 6A, June , 2002, pp. 3866-3876.

[10] D. Stansfield, *Underwater Electroacoustic Transducers*, Bath University Press and Institute of Acoustics, 1990.

[11] R. Helsel, *Visual Programming with HP VEE*, Third Edition, Hewlett-Packard Company, Published by Prentice Hall PTP, Prentice-Hall, Inc. , Asimon & Schuster Company, upper Saddle River, New Jersey 07458, 1998.

[12] T. Baumeister, *Mechanical Engineers' Hand Book*, Mcgraw-Hill, New York, 1958, pp. 95-108.

[13] Yeong-Chin Chen, Long Wu, Kuei-Kai Chang and Cheng-Liang Huang, Analysis and Simulation of Stacked-Segment Electromechanical Transducers with Partial Electrical Excitation by PSPICE, *Japanese Journal of Applied Physics*, Vol. 36, Pare 1, No. 10, October 1997, pp.6550.

[14] W. Jack Hughes, *Encyclopedia of Applied Physics*, Vol. 2, Transducer, Underwater Acoustics chapter, Wiely-VCH Verlag GmbH, 1998.

[15] IRE standards on Piezoelectric Crystal, *The Piezoelectric Vibrator Definitions and Methods of Magnet*, Published by the IEEE, New, York, 1957.

[16] D.A. Berlincourt, D.R. Curran, H. Jaffe, Pizoelectric and Piezomagnetic materials and their function in transducers, *Physical Acoustics*, Vol. 1, Part A, Academic Press, 1964.

[17] Oscar Bryan Wilson, *Introduction to Theory and Design of Sonar Transducers*, edition published by peninsula publishing, 1988.

[18] Y. C. Chen, L. Wu, K. K. Chang, C. L. Huang, PSPICE Simulation of Tonpiltz Transducer with Different Metal Material Loaded on Both Ends, *Ferroelectrics*, Vol. 220, 1999, pp. 31-42.